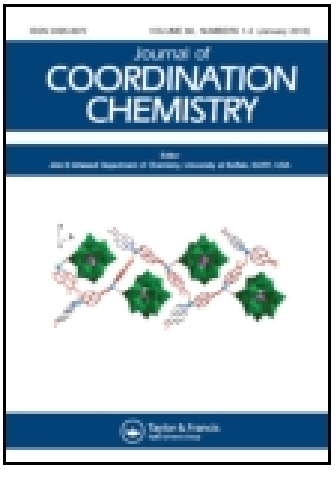

Journal of Coordination Chemistry
Publication details, including instructions for authors and subscription information:
http://www.tandfonline.com/loi/gcoo20

Synthesis, characterization, and catalytic activity of heterometallic ion-pair Ni/Mn and Ni/Zn complexes

Nittaya Thuyweang[a], Lip Lin Koh[b], T.S. Andy Hor[bc] & Somying Leelasubcharoen[a]

[a] Materials Chemistry Research Unit, Faculty of Science, Department of Chemistry and Center of Excellence for Innovation in Chemistry, Khon Kaen University, Khon Kaen, Thailand

[b] Faculty of Science, Department of Chemistry, National University of Singapore, Singapore

[c] Institute of Materials Research and Engineering, Agency for Science, Technology and Research, Singapore

Accepted author version posted online: 22 Apr 2014.Published online: 08 May 2014.

To cite this article: Nittaya Thuyweang, Lip Lin Koh, T.S. Andy Hor & Somying Leelasubcharoen (2014) Synthesis, characterization, and catalytic activity of heterometallic ion-pair Ni/Mn and Ni/Zn complexes, Journal of Coordination Chemistry, 67:7, 1219-1235, DOI: 10.1080/00958972.2014.911850

To link to this article: http://dx.doi.org/10.1080/00958972.2014.911850

Journal of Coordination Chemistry, 2014
Vol. 67, No. 7, 1219–1235, http://dx.doi.org/10.1080/00958972.2014.911850

Synthesis, characterization, and catalytic activity of heterometallic ion-pair Ni/Mn and Ni/Zn complexes

NITTAYA THUYWEANG†, LIP LIN KOH‡, T.S. ANDY HOR‡§ and SOMYING LEELASUBCHAROEN*†

†Materials Chemistry Research Unit, Faculty of Science, Department of Chemistry and Center of Excellence for Innovation in Chemistry, Khon Kaen University, Khon Kaen, Thailand
‡Faculty of Science, Department of Chemistry, National University of Singapore, Singapore
§Institute of Materials Research and Engineering, Agency for Science, Technology and Research, Singapore

(*Received 25 September 2013; accepted 11 March 2014*)

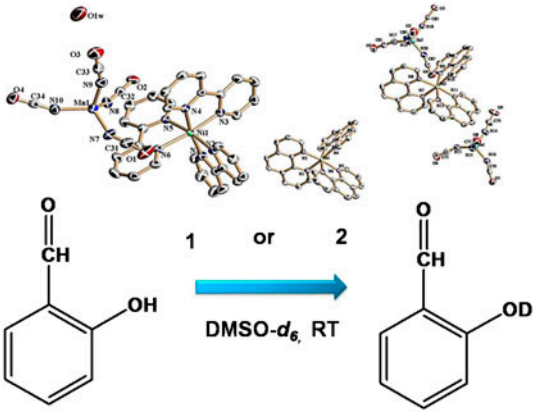

Two new heterometallic compounds, $[Ni(bpy)_3][Mn(NCO)_4]\cdot H_2O$ (**1**) and $[Ni(phen)_3]_2[Zn(NCO)_4]_2\cdot 4DMSO\cdot H_2O$ (**2**) [bpy = 2,2′-bipyridine and phen = 1,10-phenanthroline], have been synthesized and characterized. The structures of **1** and **2** were solved by single-crystal X-ray diffraction analysis. The cationic moieties of $[Ni(bpy)_3]^{2+}$ in **1** and $[Ni(phen)_3]^{2+}$ in **2** show octahedral environments around Ni(II), whereas the anionic groups of $[Mn(NCO)_4]^{2-}$ in **1** and $[Zn(NCO)_4]^{2-}$ in **2** exhibit tetrahedral geometry around the Mn(II) and Zn(II), respectively. Both compounds are catalysts in the H/D exchange of salicylaldehyde in DMSO-d_6 which takes place under mild conditions and short reaction time.

Keywords: H/D exchange reaction; Catalysis; Heterometallic complex; Ion pair; Cyanate

*Corresponding author. Email: somying@kku.ac.th

1. Introduction

Hydrogen/deuterium (H/D) exchange processes are powerful methods to evaluate the potential of a catalyst for substitution of hydrogen by solvent deuterium [1]. Hydrogens from side chains of a protein that contain –OH, –SH, $–NH_2$, –COOH, $–CONH_2$ groups, and hydrogens from amino and carboxylate termini exhibit rapid H/D exchange [2]. H/D exchange is an important method for characterizing the conformational flexibility of β_2-microglobulin amyloid fibrils at single residue resolution [3]. Furthermore, deuterated products have been found in drug discovery processes [4]. Therefore, there is interest in selective catalytic H/D exchange processes for the synthesis of deuterated products. H/D exchange reactions have been catalyzed by using acid [5], base [6], or transition metals [7]. The processes are usually performed with D_2 or in deuterated organic solvents such as benzene (C_6D_6), acetone (C_2D_6CO), deuterium oxide (D_2O), and methanol (CD_3OD), and only in very few cases dimethyl sulfoxide (C_2D_6SO) can be used [8–12]. The use of heterometallic complexes for catalyzed H/D exchange has been found in the past decade. Heterometallic systems have been studied due to the promise of enhanced catalytic reactivity from the cooperative activation and synergistic interaction of metal centers with differing electronic properties [13]. Heterometallic Rh/Pd and Rh/Pt complexes rapidly catalyze selective H/D exchange of one of the diastereotopic protons of the dipycolylamine methylene group in the presence of CD_3OD [14]. Mixed metal complexes offer the opportunity for metal–metal cooperation [15–18]. The π–π stacking interactions between parallel aromatic rings of 2,2′-bipyridine (bpy) and 1,10-phenanthroline (phen) have been exploited for coordinative assemblies [19, 20]. Recently, new ion-pair complexes containing bipyridine and 1,10-phenanthroline such as $[Ni(bpy)_3]_2[Ag(CN)_2]_3Cl{\cdot}9H_2O$ [21], $[Ni(bpy)_3][Ni(CN)_4]{\cdot}6H_2O{\cdot}0.5bpy$ [22], $[Ni(bpy)_3][Fe(CN)_5(NO)]{\cdot}3H_2O$ [23], $[Ni(bpy)_3][ZnCl(H_2PO_4)_3]$ [24], $[Ni(bpy)_3]_2[Mo(CN)_8]{\cdot}12H_2O$ [25], $[Ni(bpy)_3]_2[W(CN)_6]{\cdot}6H_2O$ [25], $[Ni(phen)_3][MnCl_4]$ [26], and $[Ni(phen)_2(tm^{t\text{-}Bu})Cl)][Zn(tm^{t\text{-}Bu})Cl_3]$ ($tm^{t\text{-}Bu}$ = 1-tert-butylimidazole-2-thione) [26] have been reported, but little is known on cyanate complexes. The present work reports the synthesis of new heterometallic compounds and a catalytic study of the compounds in the H/D exchange of salicylaldehyde in DMSO-d_6 solvent.

2. Experimental setup

2.1. *Materials and general methods*

$NiCl_2{\cdot}6H_2O$, NaOCN, and dimethyl sulfoxide (DMSO-h_6) were purchased from Sigma-Aldrich. $MnCl_2{\cdot}4H_2O$, 2,2′-bipyridine, 1,10-phenanthroline, and organic solvents were purchased from CARLO ERBA. $Ni(NO_3)_2{\cdot}6H_2O$ was purchased from QRëc. $Zn(CH_3COO)_2{\cdot}2H_2O$ was purchased from UNIVAR. Salicylaldehyde and DMSO-d_6 were purchased from Aldrich. Elemental analyses of carbon, hydrogen, and nitrogen were performed on a Perkin–Elmer model 2400 elemental analyzer. FT-IR spectra were recorded as KBr disks from 4000 to 400 cm^{-1} on a Perkin–Elmer Spectrum One FT-IR spectrophotometer. Solid-state (diffuse reflectance) electronic spectrum was measured as polycrystalline sample on a Perkin–Elmer Lambda 2s spectrometer from 8000 to 18,000 cm^{-1}. Thermogravimetric analyses were carried out on a Pyris Diamond TG-DTA, Perkin–Elmer instrument with a heating rate of 10 °C min^{-1} in a flow of nitrogen gas. Melting point was observed in a capillary tube on an Electrothermal 9100.

The progress of the reaction was monitored by ^{1}H NMR spectroscopy at 27 °C. ^{1}H NMR spectra were recorded on a Varian Mecury Plus 400 Spectrometer. The organic product was confirmed by gas chromatography–mass spectrometry (GC–MS) using a Trace GC chromatograph equipped with a Finnigan Polaris Q mass spectrometer (Thermo Finnigan, USA). About 1 µL of the sample was injected into the gas chromatograph using the splitless mode. Organic products were analyzed with a ZB-5 column (30 m × 0.25 mm i.d., 0.25 µm film thickness). The oven was programmed with step temperature program starting at 60 °C for 5 min and increased to 280 °C with a heating rate of 3 °C min^{-1}. Helium gas was used as carrier gas at a flow rate of 1.0 mL min^{-1} (constant flow). The GC injector temperature was 200 °C and the transfer line temperature was held at 275 °C. The mass spectrometer presented an electronic impact source (EI) to promote electron ionization operated at the ionization energy of 70 eV and temperature of the ion source of 250 °C.

2.2. *Synthesis of [Ni(bpy)$_3$][Mn(NCO)$_4$]·H$_2$O (1)*

A methanol solution (5.0 mL) of 2,2′-bipyridine 0.46 g (3.0 mM, 3 eq) was added to a methanol solution (5.0 mL) of $NiCl_2 \cdot 6H_2O$ 0.25g (1 mM, 1 eq). The mixture was stirred for 30 min at room temperature followed by adding a solution of NaOCN 0.15g (2.0 mM, 2 eq) in

Table 1. Crystal data and structure refinement parameters for **1** and **2**.

Complex	**1**	**2**
Empirical formula	$C_{34}H_{26}MnN_{10}NiO_5$	$C_{88}H_{74}N_{20}Ni_2O_{13}S_4Zn_2$
Formula weight	768.30	1996.07
Temperature (K)	100(2)	293(2)
Wavelength (Å)	0.71073	0.71073
Crystal system	Orthorhombic	Triclinic
Space group	*Pbcn*	*P*$\bar{1}$
a (Å)	14.3532(15)	11.0569(7)
b (Å)	19.972(2)	19.1548(11)
c (Å)	23.449(2)	21.5902(13)
α (°)	90	97.5970(10)
β (°)	90	91.0710(10)
γ (°)	90	105.0240(10)
Volume (Å^3)	6722.2(12)	4370.9(5)
Z	8	2
Density (Calcd) (Mg m^{-3})	1.518	1.517
Absorption coefficient (mm^{-1})	0.994	1.138
F (000)	3144	2052
Crystal size (mm^3)	0.48 × 0.24 × 0.22	0.56 × 0.40 × 0.20
Theta range for data collection (°)	1.74–27.49	1.11–27.50
Index ranges	$-14 \le h \le 18$, $-25 \le k \le 25$, $-30 \le l \le 29$	$-14 \le h \le 14$, $-24 \le k \le 24$, $-28 \le l \le 27$
Reflections collected	45,873	56,499
Independent reflections	7703 [*R*(int) = 0.0459]	20,062 [*R*(int) = 0.0361]
Max. and min. transmission	0.8109 and 0.6468	0.5629 and 0.4507
Refinement method	Full-matrix least-squares on F^2	Full-matrix least-squares on F^2
Data/restraints/parameters	7703/2/466	20,062/15/1177
Goodness-of-fit on F^2	1.048	1.052
Final *R* indices [$I > 2\sigma(I)$]	*R*1 = 0.0430, *wR*2 = 0.1020	*R*1 = 0.0448, *wR*2 = 0.1123
R indices (all data)	*R*1 = 0.0548, *wR*2 = 0.1073	*R*1 = 0.0564, *wR*2 = 0.1178
Largest diff. peak and hole (e Å^{-3})	0.644 and −0.750	1.345 and −0.900

deionized water (5.0 mL). After stirring for 30 min, a methanol solution of $MnCl_2{\cdot}4H_2O$ 0.20 g (1 mM, 1 eq) was added to the solution and stirred for another 5 h. Red powder precipitated and was recrystallized in DMSO. Red crystals were obtained after three days by slow evaporation at room temperature. Yield = 0.47 g (70%). M.p. >250 °C. FT-IR (KBr, cm^{-1}): 3508 (br), 3081 (w), 2188(s), 1599 (m), 1493 (m), 770 (s) and 621 (m). Anal. Calcd for $NiMnC_{34}H_{26}N_{10}O_5$: C, 53.15; H, 3.41; N, 18.23%. Found: C, 53.02; H, 3.22; N, 17.73%.

2.3. *Synthesis of $[Ni(phen)_3]_2[Zn(NCO)_4]_2{\cdot}4DMSO{\cdot}H_2O$ (2)*

About 5.0 mL of methanol solution of 1,10-phenanthroline 0.30 g (1.5 mM, 3 eq) was added to a methanol solution (5.0 mL) of $Ni(NO_3)_2{\cdot}6H_2O$ 0.16 g (0.5 mM, 1 eq). The mixture was stirred for 30 min at room temperature followed by adding a solution of NaOCN 0.07 g (1.0 mM, 2 eq) in 5.0 mL of DI. After the mixture was stirred for 30 min, a methanol solution of $Zn(OAc)_2{\cdot}2H_2O$ 0.15 g (0.5 mM, 1 eq) was added to the mixture and stirred for 5 h. Red powder precipitated and was recrystallized in DMSO. Red crystals appeared in three days by slow evaporation at room temperature. Yield = 73.75%. M.p. >250 °C. Anal. Calcd for $Ni_2Zn_2C_{88}H_{74}N_{20}O_{13}S_4$: C, 52.95; H, 3.74; N, 14.03%. Found: C, 53.17; H, 3.53; N, 14.75%. IR (KBr, cm^{-1}): 3445 (br), 3062 (w), 2208 (s), 1626 (m), 1426 (m), 848 (s), 726 (s).

2.4. *Catalytic reaction*

$[Ni(bpy)_3][Mn(NCO)_4]{\cdot}H_2O$ (**1**) 0.0029 g (0.0038 mM, 3 M%) was dissolved in DMSO-d_6 (ca. 0.4 mL) and transferred into an NMR tube. Salicylaldehyde 13.40 μL (0.1260 mM) was injected into the tube and determined by ^1H NMR spectroscopy. The progress of the reaction was monitored by ^1H NMR spectroscopy. The product of the H/D exchange reaction was identified by GC–MS analysis. ^1H NMR(DMSO-d_6, ppm) δ: 10.23 (1H, CH), 7.65 (1H, Ar–H), 7.49 (1H, Ar–H), 6.98 (2H, Ar–H). EI-MS (70 eV): *m/z* (rel. int. %): 123(23), 121(100), 65(16).

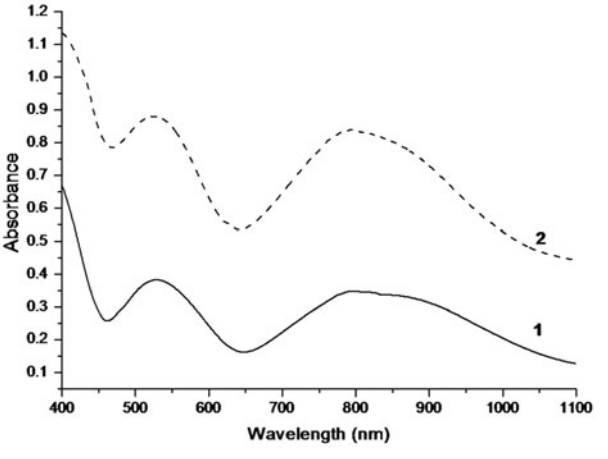

Figure 1. Diffuse reflectance spectra of **1** and **2**.

$[Ni(phen)_3]_2[Zn(NCO)_4]_2 \cdot 4DMSO \cdot H_2O$ (**2**) 0.0076 g (0.0038 mM, 3 M%), $Zn(OAc)_2 \cdot 2H_2O$ 0.0008 g (0.0038 mM, 3 M%), $Ni(NO_3)_2 \cdot 6H_2O$ 0.0011 g (0.0038 mM, 3 M%), $NiCl_2 \cdot 6H_2O$ 0.0011 g (0.0038 mM, 3 M%), or $MnCl_2 \cdot 4H_2O$ 0.0008 g (0.0038 mM, 3 M%) were used as catalysts in identical reactions.

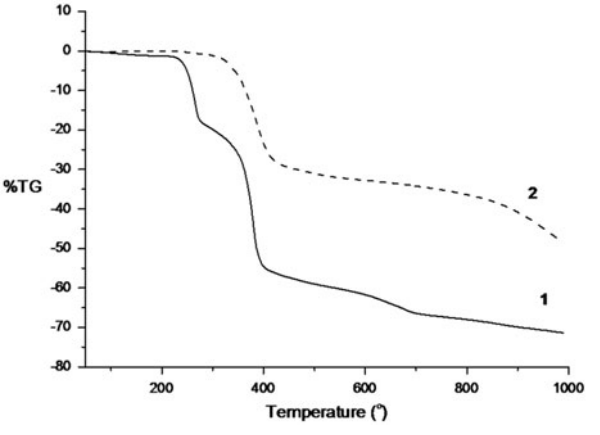

Figure 2. TGA curves of **1** and **2**.

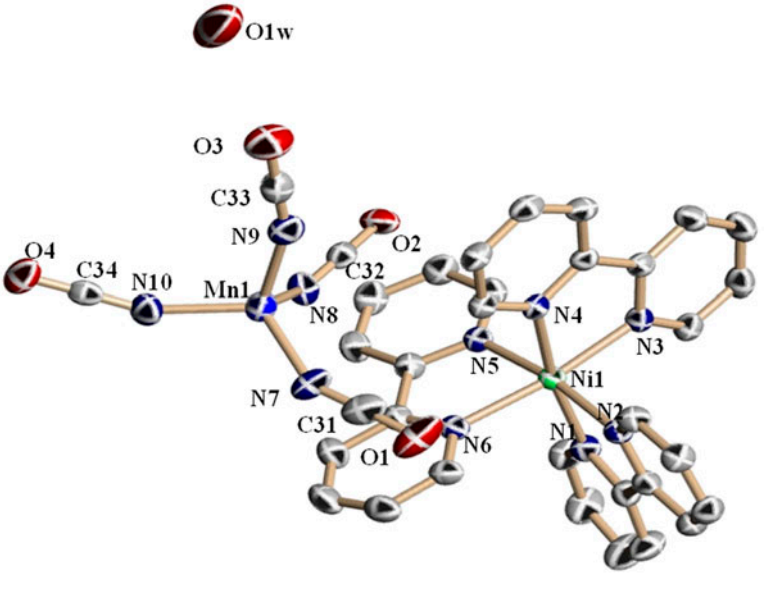

Figure 3. Molecular structure of $[Ni(bpy)_3][Mn(NCO)_4] \cdot H_2O$ (**1**) with displacement ellipsoids shown at 50% probability level.

Table 2. Selected bond lengths (Å) and angles (°) for **1** and **2**.

1		**2**	
Bond lengths (Å)		Bond lengths (Å)	
Ni(1)–N(1)	2.0842(19)	Ni(1)–N(6)	2.0744(18)
Ni(1)–N(2)	2.0800(19)	Ni(1)–N(3)	2.0799(17)
Ni(1)–N(3)	2.075(2)	Ni(1)–N(2)	2.0833(18)
Ni(1)–N(4)	2.0806(19)	Ni(1)–N(1)	2.0869(18)
Ni(1)–N(5)	2.0774(19)	Ni(1)–N(4)	2.1019(18)
Ni(1)–N(6)	2.093(2)	Ni(1)–N(5)	2.1170(18)
Mn(1)–N(7)	2.067(2)	Ni(2)–N(12)	2.0733(18)
Mn(1)–N(8)	2.073(2)	Ni(2)–N(9)	2.0789(17)
Mn(1)–N(9)	2.067(3)	Ni(2)–N(8)	2.0803(17)
Mn(1)–N(10)	2.040(2)	Ni(2)–N(7)	2.0868(18)
		Ni(2)–N(11)	2.0927(18)
Bond angles (°)			
N(5)–Ni(1)–N(2)	169.92(8)	Ni(2)–N(10)	2.1205(17)
N(4)–Ni(1)–N(1)	171.27(7)	Zn(1)–N(13)	1.959(2)
N(3)–Ni(1)–N(6)	171.95(7)	Zn(1)–N(14)	1.960(2)
N(10)–Mn(1)–N(9)	103.66(10)	Zn(1)–N(15)	1.967(2)
N(10)–Mn(1)–N(7)	113.64(10)	Zn(1)–N(16)	1.992(2)
N(9)–Mn(1)–N(7)	110.13(10)	Zn(2)–N(17)	1.956(2)
N(10)–Mn(1)–N(8)	112.44(9)	Zn(2)–N(18)	1.9619(19)
N(9)–Mn(1)–N(8)	106.14(9)	Zn(2)–N(19)	1.970(2)
N(7)–Mn(1)–N(8)	110.35(9)	Zn(2)–N(20)	1.977(2)
N(7)–C(31)–O(1)	178.7(4)	N(1)–C(1)	1.331(3)
N(8)–C(32)–O(2)	177.8(3)	N(1)–C(12)	1.356(3)
N(9)–C(33)–O(3)	178.8(3)	N(13)–C(73)	1.162(3)
N(10)–C(34)–O(4)	179.5(3)	N(14)–C(75)	1.165(3)
		N(15)–C(77)	1.165(3)
		N(16)–C(79)	1.175(3)
		N(17)–C(81)	1.162(3)
		N(20)–C(87)	1.158(3)
		N(18)–C(83)	1.169(3)

2		Bond angles (°)	
Bond lengths (Å)		N(19)–Zn(2)–N(20)	109.56(12)
N(19)–C(85)	1.169(3)	C(73)–N(13)–Zn(1)	154.94(19)
		C(75)–N(14)–Zn(1)	170.8(2)
Bond angles (°)		C(77)–N(15)–Zn(1)	148.6(2)
N(8)–Ni(2)–N(11)	172.52(7)	C(79)–N(16)–Zn(1)	147.11(19)
N(7)–Ni(2)–N(10)	172.86(7)	C(81)–N(17)–Zn(2)	164.58(19)
N(12)–Ni(2)–N(9)	168.32(7)	C(83)–N(18)–Zn(2)	165.1(2)
N(2)–Ni(1)–N(5)	172.72(7)	C(85)–N(19)–Zn(2)	143.9(2)
N(1)–Ni(1)–N(4)	172.31(7)	C(87)–N(20)–Zn(2)	158.9(2)
N(6)–Ni(1)–N(3)	167.91(7)	N(19)–Zn(2)–N(20)	109.56(12)
N(14)–Zn(1)–N(15)	110.50(9)	C(73)–N(13)–Zn(1)	154.94(19)
N(13)–Zn(1)–N(16)	111.44(8)		
N(14)–Zn(1)–N(16)	106.81(9)		
N(15)–Zn(1)–N(16)	107.27(9)		
N(17)–Zn(2)–N(18)	110.97(8)		
N(17)–Zn(2)–N(19)	109.36(10)		
N(18)–Zn(2)–N(19)	107.99(10)		
N(19)–Zn(2)–N(20)	109.56(12)		
C(73)–N(13)–Zn(1)	154.94(19)		
C(75)–N(14)–Zn(1)	170.8(2)		
C(77)–N(15)–Zn(1)	148.6(2)		
C(79)–N(16)–Zn(1)	147.11(19)		
C(81)—N(17)–Zn(2)	164.58(19)		
C(83)–N(18)–Zn(2)	165.1(2)		
C(85)–N(19)–Zn(2)	143.9(2)		
C(87)–N(20)–Zn(2)	158.9(2)		

2.5. *X-ray crystallography*

Crystals of **1** and **2** suitable for X-ray crystallographic analysis were obtained from slow evaporation of a DMSO solution at room temperature. Red block-shaped crystals of **1** and **2** were mounted on quartz fibers for data collection. Diffraction data were collected on a Brüker AXS APEX diffractometer, equipped with a CCD detector, using graphite-monochromated Mo Kα radiation ($\lambda = 0.71073$ Å). The collecting frames of data, indexing reflection, and determination of lattice parameters and polarization effects were performed with the SMART suite of programs. Integration of intensity of reflections and scaling was performed by SAINT [27] and empirical absorption correction was performed by SADABS [28]. Space group determination, structure solution, and least-squares refinements on $|F|^2$ were carried out with SHELXTL [29]. The crystal and refinement data of **1** and **2** are listed in table 1.

3. Results and discussion

3.1. *Synthesis and spectroscopic characterization of 1 and 2*

New heterometallic products **1** and **2** were synthesized by a direct method under mild conditions. Compound **1** shows a broad adsorption at 3508 cm^{-1} due to O–H stretch of water. The strong peak at 2188 cm^{-1} is assigned to C=N stretch of cyanate [30]. Medium peaks at 1599 cm^{-1} are attributed to C=N stretch, whereas a medium peak at 770 cm^{-1} is assigned to C–H stretch. This result is assigned to pyridine ring stretching vibrations [24]. Compound **2** shows a broad peak at 3445 cm^{-1}, attributed to O–H stretch of water. The strong peak at 2208 cm^{-1} is assigned to C=N stretch of cyanate [30]. The medium peak at 1626 cm^{-1} is attributed to C=N stretch and the medium peak at 726 cm^{-1} is assigned to C–H stretch. The electronic spectra of **1** and **2** are represented in figure 1. The two

Table 3. The comparison of the bond distances (Å) and angles (°) of cations of **1** and **2** with previous research.

Complexes	Bond distances of Ni–N	Bond angles of N–Ni-N	Ref.
$[Ni(bpy)_3]_2[Ag(CN)_2]_3Cl{\cdot}9H_2O$	2.093(3)–2.096(3)	78.46(10)–95.28 (10)	[21]
$[Ni(bpy)_3][Ni(CN)_4]{\cdot}6H_2O{\cdot}0.5bpy$	2.078(3)–2.100(3)	78.72(11)–79.14(11)	[22]
$[Ni(bpy)_3][Fe(CN)_5(NO)]{\cdot}3H_2O$	2.072(3)–2.103(3)	94.35(13)–95.77(13)	[23]
$[Ni(bpy)_3][ZnCl(H_2PO_4)_3]$	2.085(5)–2.089(6)	78.7(2)–94.8(2)	[24]
$[Ni(bpy)_3]_2[Mo(CN)_8]{\cdot}12H_2O$	2.062(13)–2.118(11)	78.5(5)–96.9(5)	[25]
$[Ni(bpy)_3]_2[W(CN)_6]{\cdot}6H_2O$	2.039(16)–2.129(16)	79.2(6)–95.7(6)	[25]
$[Ni(phen)_3][MnCl_4]$	2.063(2)–2.144(3)	79.49(8)–96.39(6)	[26]
$[Ni(bpy)_3][Mn(NCO)_4]{\cdot}H_2O$ (**1**)	2.075(2)–2.093(2)	78.76(8)–95.35(7)	This work
$[Ni(phen)_3]_2[Zn(NCO)_4]_2{\cdot}4DMSO{\cdot}H_2O$ (**2**)	2.0744(18)–2.1170(18)	79.57(7)–96.24(7)	This work

Table 4. Hydrogen bonds (Å) and angles (°) for $[Ni(bpy)_3][Mn(NCO)_4]{\cdot}H_2O$ (**1**).

D–H···A	d(D–H)	d(H···A)	d(D···A)	∠(DHA)
O(1W)–H(1WB)···O(1)^{i}	0.928(19)	1.92(4)	2.743(4)	146(5)
O(1W)–H(1WA)···O(3)	0.927(19)	1.87(3)	2.737(4)	154(5)

Note: Symmetry transformations used to generate equivalent atoms, i: $-x+1/2, -y+1/2, z-1/2$.

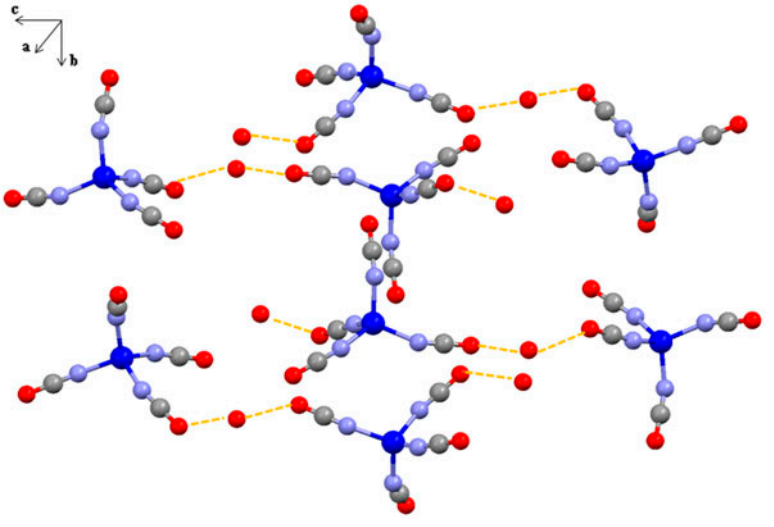

Figure 4. The hydrogen bonded (dashed lines) chain between water and $[Mn(NCO)_4]^{2-}$, showing the 1-D chain along the *c* axis. The $[Ni(bpy)_3]^{2+}$ has been omitted for clarity [symmetry code, i: $-x+1/2, -y+1/2, z-1/2$].

absorptions peaks occur at 526 and 793 nm for **1** which is similar to **2** (525 and 800 nm). Two absorption bands are assigned as the $^3A_{2g}$ to $^3T_{1g}(F)(\nu_2)$ and $^3A_{2g}$ to $^3T_{2g}(F)(\nu_1)$ transitions, respectively. The absorption band of the $^3A_{2g}$ to $^3T_{1g}(p)(\nu_3)$ transition is obscured by the charge transfer band of the diimine ligand. The visible transitions are described as *d–d* transitions of the nickel(II) in near octahedral environment [26].

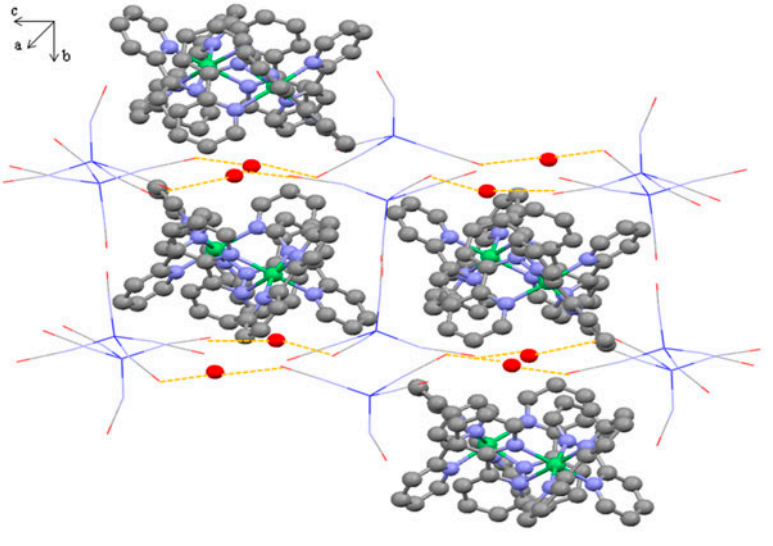

Figure 5. The crystal packing of $[Ni(bpy)_3][Mn(NCO)_4]\cdot H_2O$ (**1**). $[Ni(bpy)_3]^{2+}$ resides in the vacancies between anion chains.

3.2. *Thermogravimetric analysis*

Thermogravimertric analyses (TGA) of both complexes were carried out on a polycrystalline sample. For **1**, the total weight loss of 65.0% takes place from 184 to 689 °C (figure 2 (solid line)). The decomposition of the compound occurs in two steps, the first of 18.5% (Calcd 18.9%) corresponds to loss of one water and three cyanates at 184–297 °C. The second drop of 46.4% (Calcd 46.1%) corresponds to loss of one cyanate and two bpy molecules at 297–689 °C. The thermal decomposition of **2** takes place in one step (figure 2 (dashed line)). The observed weight loss of 31.68% (Calcd 32.16%) corresponds to loss of two 1,10-phenanthroline, one cyanate, two dimethyl sulfoxide, and one water from 217 to 530 °C.

3.3. *Crystallographic structure*

3.3.1. Crystal structure of $[Ni(bpy)_3][Mn(NCO)_4]\cdot H_2O$ (1). Complex **1** is ionic and consists of a $[Ni(bpy)_3]^{2+}$, $[Mn(NCO)_4]^{2-}$, and a water hydrate (figure 3). Selected bond distances and angles are given in table 2. The $[Ni(bpy)_3]^{2+}$ is six-coordinate with three chelating bpy. The Ni–N bond distances are 2.075(2)–2.093(2) Å and in agreement with the literature value [20–24]. The coordination sphere is slightly distorted from ideal octahedral, with N–Ni–N_{trans} angles varying from 169.92(8)° to 171.95(7)°. The comparison of the bond distances and bond angles of the cationic moiety with the previous reports is shown

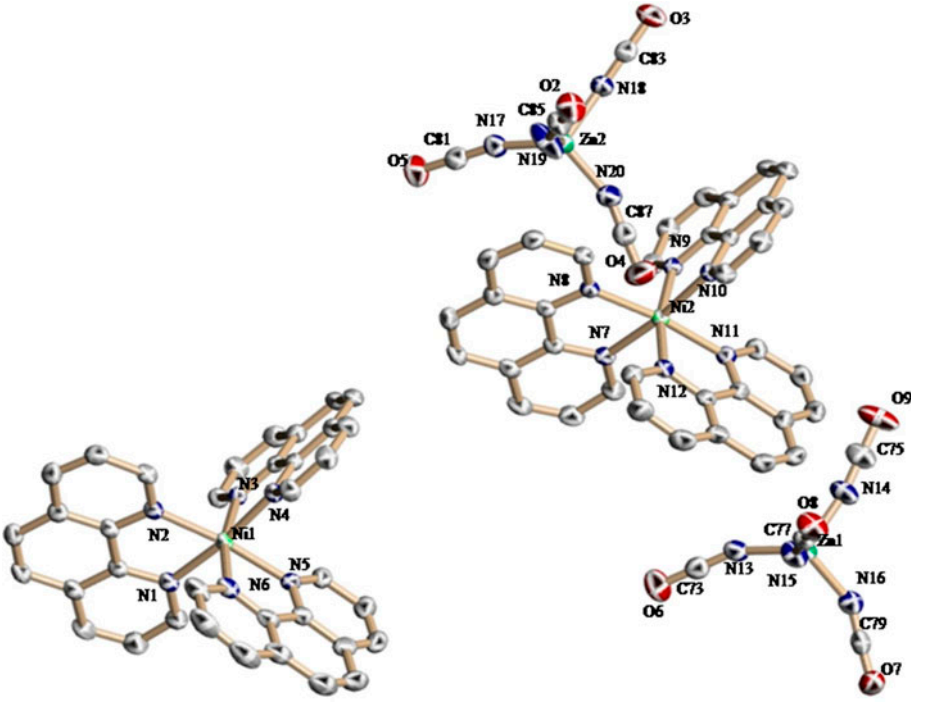

Figure 6. The molecular structure of $[Ni(phen)_3]_2[Zn(NCO)_4]_2\cdot 4DMSO\cdot H_2O$ (**2**) with displacement ellipsoids shown at 50% probability level.

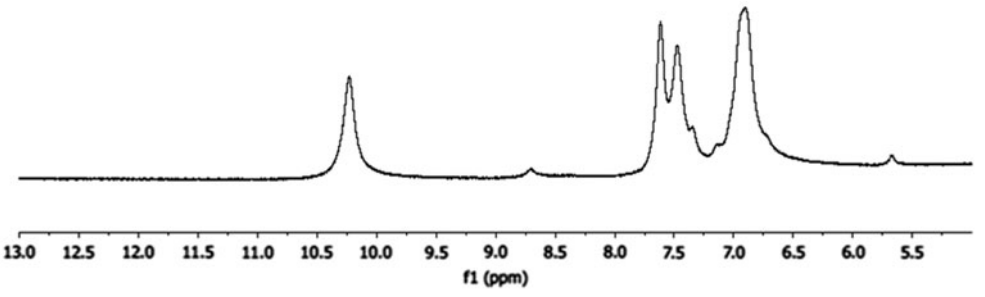

Figure 7. ^{1}H NMR spectrum of salicylaldehyde-d_1 in the presence of **1**.

in table 3. The data of **1** insignificantly differ from those in previous work, which confirms the octahedral geometry. $[Mn(NCO)_4]^{2-}$ is tetrahedral with manganese(II) coordinated with four N-donating cyanate groups. The same anion was reported in $(Et_4N)_2Mn(NCO)_4$ but this complex has not been crystallographically characterized [31]. The Mn–N bond distances are within the range of 2.040(2) to 2.073(2) Å, similar to the literature values of 2.105(2) Å for $[Mn(salen)(NCO)]_2$ [32]. The N–Mn–N bond angles vary from 103.16(10)°

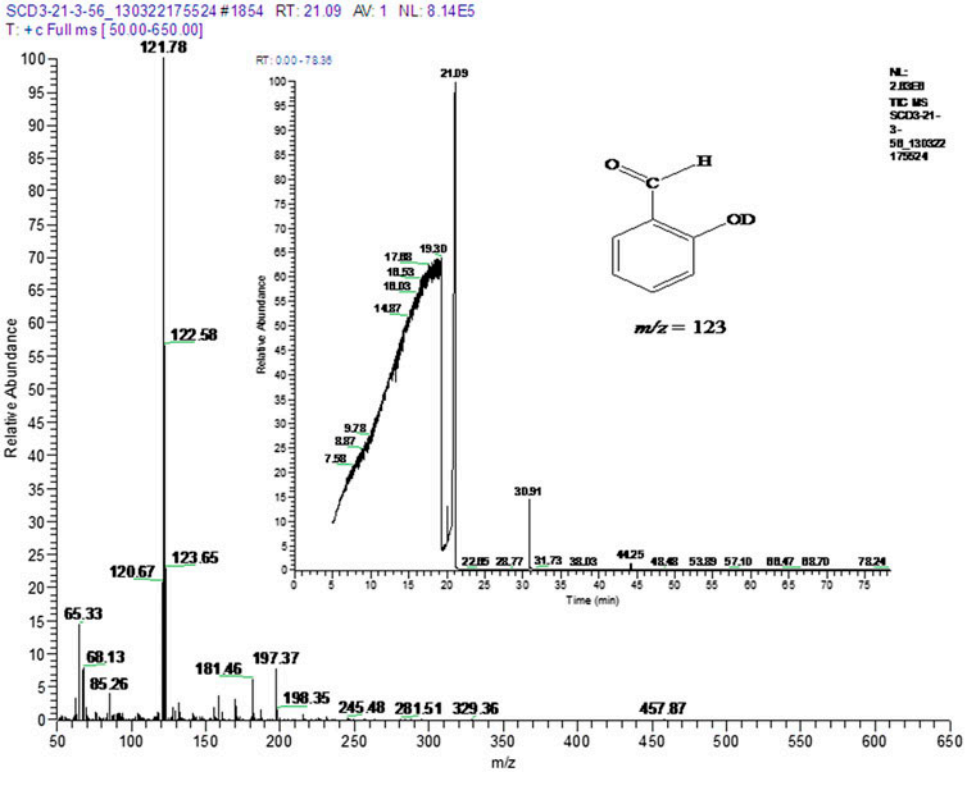

Figure 8. GC–MS chromatogram of salicylaldehyde in DMSO-d_6 in the presence of **1**.

to 112.44(9)° within a tetrahedral geometry. The cyanates are linear, as evident from N–C–O angles (178.8(3)°–179.5(3)°). In addition, each water is involved in two hydrogen bonds, formed between hydrogen of water and oxygen of cyanate. The bond distances of O(1W)···O1^{i} and O(1W)···O3 are 2.743(4) and 2.737(4) Å, respectively. The bond angles for O(1W)–H(1WB)···O1^{i} and O(1W)–H(1WA)···O3 are 146(5)° and 154(5)°, respectively (table 4). These H-bonding interactions stabilize the structure by linking the dianions and extending into a 1-D chain along the *c* axis (figure 4). As shown in the crystal packing, $[Ni(bpy)_3]^{2+}$ reside in the vacancies between the anion chains (figure 5).

3.3.2. Crystal structure of $[Ni(phen)_3]_2[Zn(NCO)_4]_2\cdot 4DMSO\cdot H_2O$ (2). Molecular structure of **2** is shown in figure 6 and selected bond distances and angles of **2** are reported in table 2. Complex **2** is an ion-pair compound built from two $[Ni(phen)_3]^{2+}$ and two $[Zn(NCO)_4]^{2-}$ along with four DMSO and one water as solvents of crystallization in the asymmetric unit. Two nickel(II) centers are chelated by phen. The Ni–N distances are 2.0744(18)–2.1170(18) and 2.0733(18)–2.1205(17) Å in Ni(1) and Ni(2), respectively. These bond distances correspond to Ni–N bond distances in $[Ni(phen)_3][MnCl_4]$ (2.063(2)–2.144(3) Å) (table 3) [26]. The N–Ni–N_{trans} bond angles are 167.91(7)°–172.52(7)°, in agreement with the literature values [26]. These values deviate from 180 ° due to steric

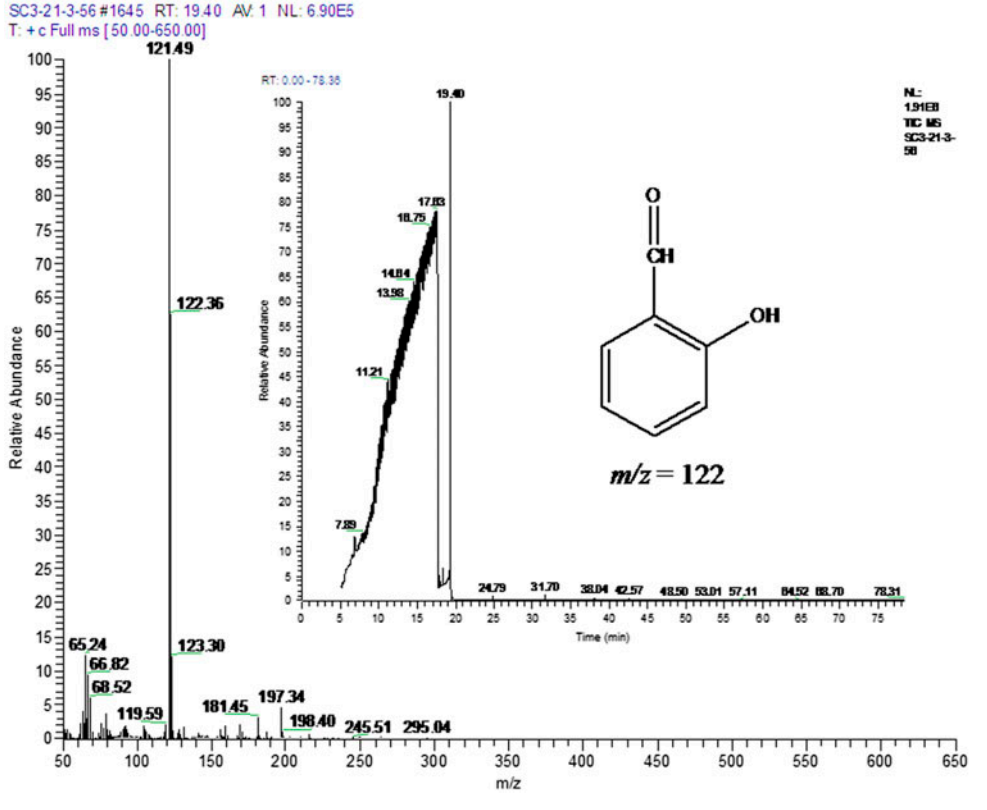

Figure 9. GC–MS chromatogram of salicylaldehyde in DMSO-h_6 in the presence of **1**.

constraints arising from the shape of the ligand. From table 3, the bond distances and bond angles of the cationic group correspond to those of the previous reports which support octahedral geometry. The Zn–N bond distances for $[Zn(NCO)_4]^{2-}$ are within the ranges 1.959 (2)–1.992(2) Å and 1.956(2)–1.977(2) Å in Zn(1) and Zn(2), respectively. The results correspond to literature values of Zn–N bond distances (1.985(6) Å) [33]. The N-Zn-N_{trans} bond angles are 106.81(9)–111.44(8)°, suggesting tetrahedral geometry [34].

3.4. *Catalytic activity*

The H/D exchange of salicylaldehyde in the presence of **1** or **2** was studied at room temperature. The reaction was monitored using ^{1}H NMR spectroscopy. The hydroxyl proton peak at 10.67 ppm disappeared within 5 min and other peaks remained unchanged in the presence of **1** (figure 7). This reaction indicates H/D exchange of salicylaldehyde. To confirm the catalytic product, GC–MS analysis was carried out. As shown in figure 8, the product ion mass spectrum of *m/z* 123 at retention time 21.09 min produces fragment ions at *m/z* 121 and 65. The ion at *m/z* 121 resulted from loss of a deuterium from fragment ion at *m/z* 123. The ion at *m/z* 65 corresponds to formation of $[M\text{-}C_5H_5]^+$. Based on the molecular weight information of salicylaldehyde, which has a m_w of 122, an increase of 1 Da suggests that only 1 active H in its structure is exchanged with deuterium. The identical reaction was also studied by using DMSO-h_6. The product ion mass spectrum of *m/z* 122 at the retention time of 19.40 min shows fragment ions at *m/z* 121 and 65 (figure 9). The ion at *m/z* 121 is formed by losing a hydrogen from the fragment ion at *m/z* 122. The presence of the fragment ion at *m/z* 65 suggests the formation of $[M\text{-}C_5H_5]^+$. This result corresponds to the free salicylaldehyde which has a m_w of 122.

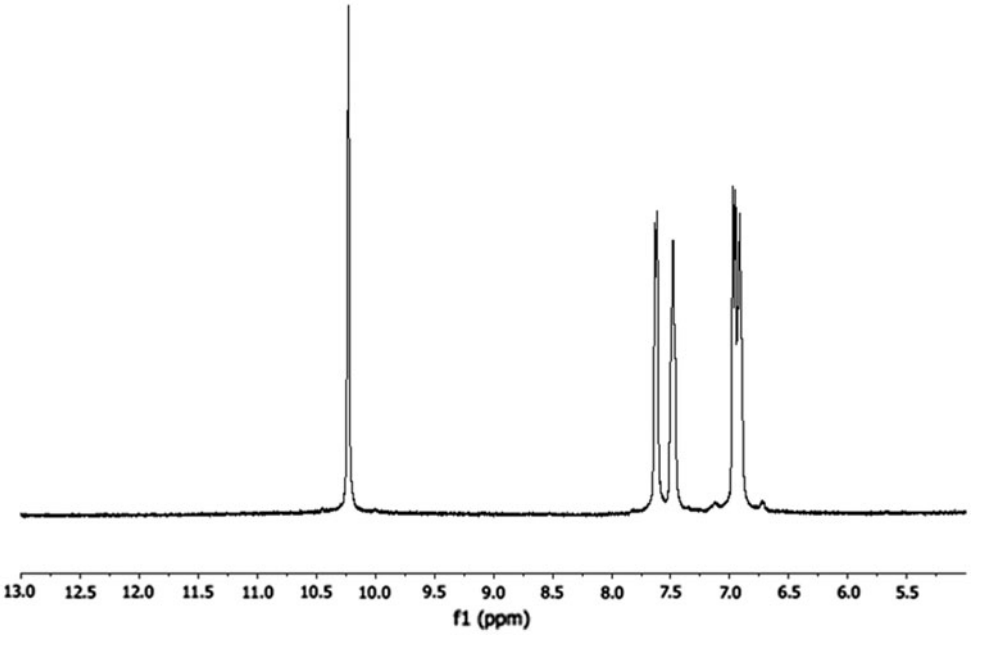

Figure 10. ^{1}H NMR spectrum of salicylaldehyde-d_1 in the presence of **2**.

The molecular weight of the salicylaldehyde increases 1 Da resulting in the slow mobility of the substance and an increase of the retention time [35]. The GC–MS analysis and ^{1}H NMR spectroscopy also confirm the H/D exchange reaction. **2** was also used as a catalyst in the H/D exchange reaction. From ^{1}H NMR data (figure 10), the proton peak at 10.67 ppm completely disappeared within 5 min. In addition, the GC–MS chromatogram of the reaction in DMSO-d_6 appeared at retention time of 19.07 min (figure 11). When DMSO-h_6 was used instead of DMSO-d_6, the GC–MS chromatogram of the reaction occurred at the retention time of 17.12 min (figure 12). Chromatogram patterns are similar to those of the reaction in the presence of **1** which was described previously. A proposed mechanism for the H/D exchange reaction of salicylaldehyde is shown in figure 13. The salicylaldehyde is coordinated to the catalyst generating **A**. After that, oxygen of DMSO abstracts a proton from the hydroxyl group of salicylaldehyde to form **B** [36]. Subsequently, the oxyanionic site abstracts a deuterium from DMSO yielding the deuterated products **C** and **D**. Heterometallic compounds dissolved in DMSO should be dissociated into $[Ni(bpy)_3]^{2+}$ and $[Mn(NCO)_4]^{2-}$ for **1** and $[Ni(phen)_3]^{2+}$ and $[Zn(NCO)_4]^{2-}$ for **2**. Considering the steric effect of the metal center, which resulted in the catalytic activity, the tetrahedral geometry of the anion is less sterically crowded than the octahedral geometry of the cation, which should be the active site for the catalysis. In addition, both bpy and phen are bidentate ligands and unlikely to dissociate giving a vacant site for the substrate to coordinate. To test the role of the catalytic part, $[Ni(bpy)_3]Cl_2{\cdot}5.5H_2O$ [37] and $[Ni(phen)_3]Cl_2{\cdot}7H_2O$ [38] were

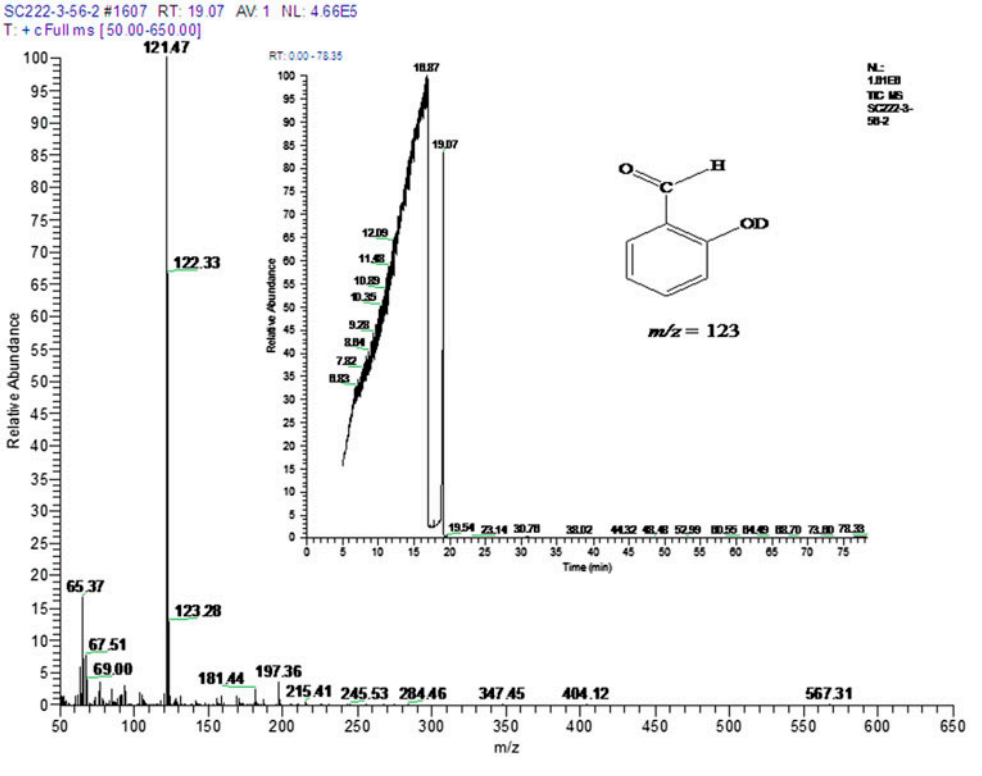

Figure 11. GC–MS chromatogram of salicylaldehyde in DMSO-d_6 in the presence of **2**.

synthesized and used in the catalytic reaction. From ^{1}H NMR spectra, the O–H peak of salicylaldehyde is unchanged after 5 h, suggesting that the anionic moiety plays the key role in the catalytic process. The same ion of **1** and **2** in previous reports, such as $[Ni(bpy)_3]_2[Ag(CN)_2]_3Cl{\cdot}9H_2O$ [21], $[Ni(bpy)_3][Ni(CN)_4]{\cdot}6H_2O{\cdot}0.5bpy$ [22], $[Ni(bpy)_3][Fe(CN)_5(NO)]{\cdot}3H_2O$ [23], $[Ni(bpy)_3][ZnCl(H_2PO_4)_3]$ [24], $[Ni(bpy)_3]_2[Mo(CN)_8]{\cdot}12H_2O$ [25], $[Ni(bpy)_3]_2[W(CN)_6]{\cdot}6H_2O$ [25], and $[Ni(phen)_3][MnCl_4]$ [26], have not been studied in catalysis.

However, reaction without complex shows no reaction even after 24 h at room temperature. In order to test the efficiency of the metal salts, the catalytic ability of various metal salts were examined for the H/D exchange of salicylaldehyde. ^{1}H NMR spectra are shown in figure 14 and the results are summarized in table 5. The reaction in the presence of $Zn(OAc)_2{\cdot}2H_2O$ takes place immediately, suggested from the decrease in the intensity of the hydroxyl proton peak. After 6 h, the hydroxyl proton peak remains as a broad peak. The identical reaction in the presence of $Ni(NO_3)_2{\cdot}6H_2O$, $NiCl_2{\cdot}6H_2O$ or $MnCl_2{\cdot}4H_2O$ shows no catalytic ability. The hydroxyl proton of salicylaldehyde remains unchanged. From the result, heterometallic compounds **1** and **2** are efficient catalysts in the H/D exchange of salicylaldehyde under mild conditions and short reaction times.

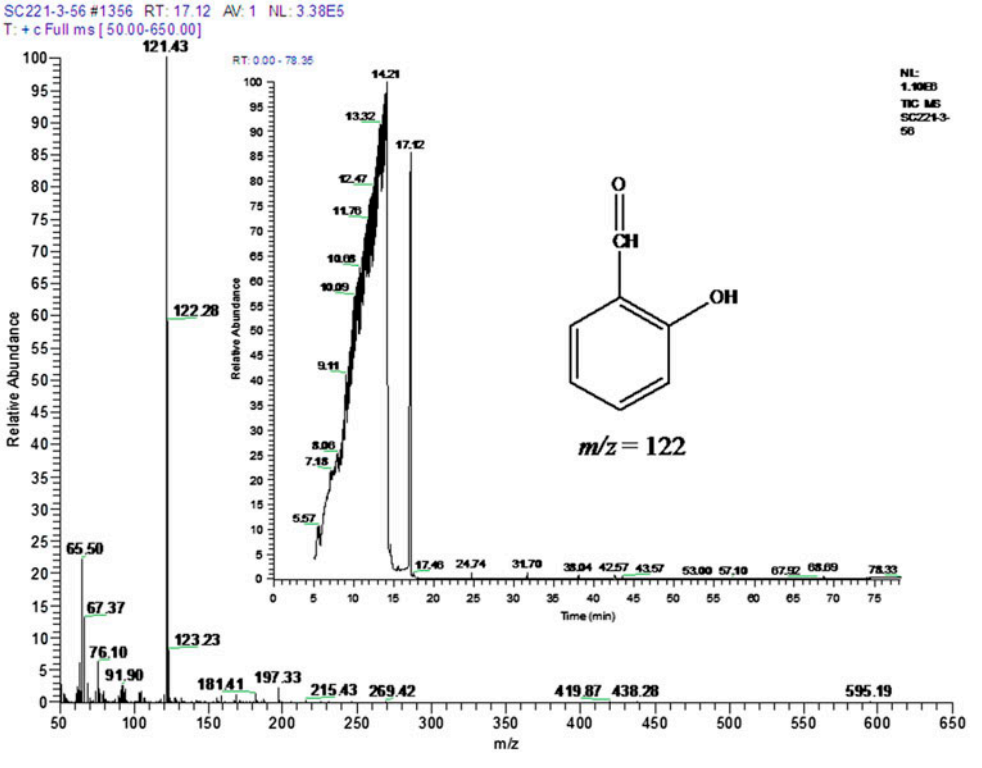

Figure 12. GC–MS chromatogram of salicylaldehyde in DMSO-h_6 in the presence of **2**.

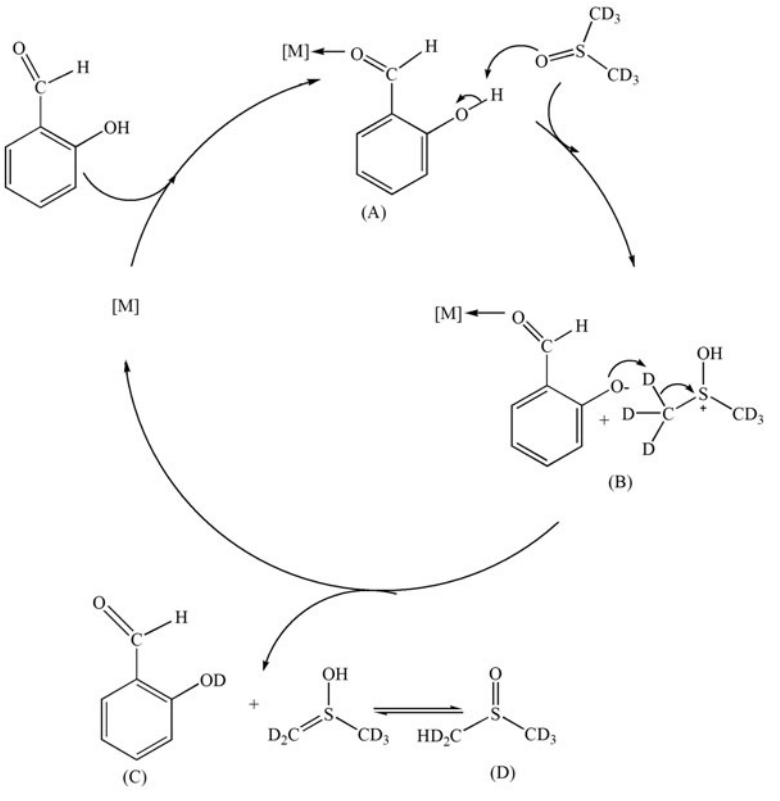

Figure 13. A proposed mechanism for the H/D exchange reaction of salicylaldehyde.

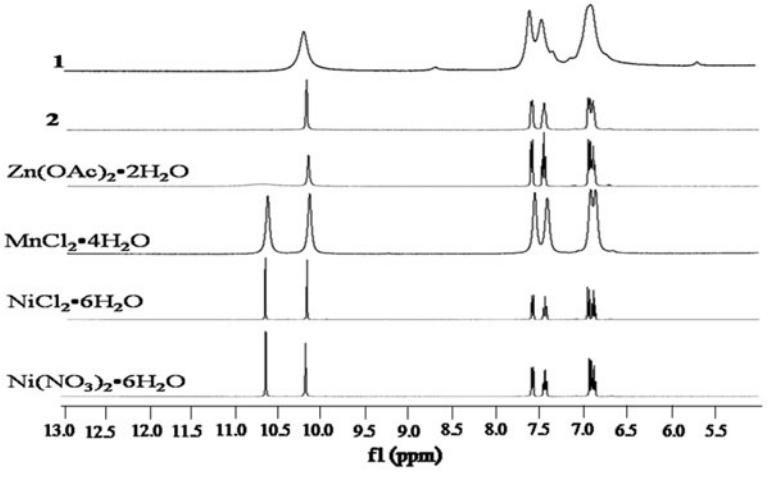

Figure 14. The ^{1}H NMR spectra of the H/D exchange of salicylaldehyde in the presence of **1**, **2**, $Zn(OAc)_2{\cdot}2H_2O$, $MnCl_2{\cdot}4H_2O$, $NiCl_2{\cdot}6H_2O$, or $Ni(NO_3)_2{\cdot}6H_2O$.

Table 5. The H/D exchange reaction of salicylaldehyde in the presence of **1**, **2**, $Zn(OAc)_2 \cdot 2H_2O$, $MnCl_2 \cdot 4H_2O$, $NiCl_2 \cdot 6H_2O$ or $Ni(NO_3)_2 \cdot 6H_2O$.

Entry	Catalysts	Time
1	$[Ni(bpy)_3][Mn(NCO)_4] \cdot H_2O$ (**1**)	5 min
2	$[Ni(phen)_3]_2[Zn(NCO)_4]_2 \cdot 4DMSO \cdot H_2O$ (**2**)	5 min
3	$Zn(OAc)_2 \cdot 2H_2O$	5 min, within 6 h peak at 10.67 ppm shows a broad
4	$MnCl_2 \cdot 4H_2O$	No reaction
5	$NiCl_2 \cdot 6H_2O$	No reaction
6	$Ni(NO_3)_2 \cdot 6H_2O$	No reaction

Note: Condition: Catalyst 3 M% in DMSO-d_6, salicylaldehyde 0.0126 mM.

4. Conclusion

Two new heterometallic compounds, $[Ni(bpy)_3][Mn(NCO)_4] \cdot H_2O$ (**1**) and $[Ni(phen)_3]_2[Zn(NCO)_4]_2 \cdot 4DMSO \cdot H_2O$ (**2**), were synthesized under mild conditions. The cationic moieties of $[Ni(bpy)_3]^{2+}$ and $[Ni(phen)_3]^{2+}$ show octahedral geometry, whereas the anionic $[Mn(NCO)_4]^{2-}$ and $[Zn(NCO)_4]^{2-}$ exhibit tetrahedral geometry. The two compounds are powerful catalysts in the H/D exchange of salicylaldehyde in a DMSO-d_6 under mild conditions and short reaction times.

Supplementary material

CCDC 882848 and 936776 contain the crystallographic data for **1** and **2**, respectively. These data can be obtained free of charge from The Cambridge Crystallographic Data Center via E-mail: deposit@ccdc.cam.ac.uk or www.ccdc.cam.ac.uk/data_request/cif.

Acknowledgements

This work was financially supported by Khon Kaen University under Incubation Researcher Project and the Center of Excellence for Innovation in Chemistry (PERCH-CIC). We are grateful to Miss Tan Geok Kheng and Hong Yimian (National University of Singapore) for the solution of the crystal structure. We wish to acknowledge the support of the Khon Kaen University Publication Clinic, Research and Technology Transfer Affairs, Khon Kaen University, for their assistance.

References

[1] M.H.G. Prechtl, M. Hölscher, Y. Ben-David, N. Theyssen, R. Loschen, D. Milstein, W. Leitner. *Angew. Chem. Int. Ed.*, **46**, 2269 (2007).
[2] Y. Hamuro, S.J. Coales, M.R. Southern, J.F. Nemeth-Cawley, D.D. Stranz, P.R. Griffin. *J. Biomol. Tech.*, **14**, 171 (2003).
[3] M. Hoshino, H. Katou, Y. Hagihara, K. Hasegawa, H. Naiki, Y. Goto. *Nature Struct. Biol.*, **9**, 332 (2002).
[4] N. Modutlwa, T. Maegawa, Y. Monguchi, H. Sajiki. *J. Labelled Comp. Radiopharm.*, **53**, 686 (2010).
[5] N. Essayem, G. Coudurier, J.C. Vedrine, D. Habermacher, J. Sommery. *J. Catal.*, **183**, 292 (1999).
[6] S. Chandrasekhar, P. Karri. *Tetrahedron Lett.*, **47**, 5763 (2006).
[7] T. Tachiyama, M. Yoshida, T. Aoyagi, S. Fukuzumi. *J. Phys. Org. Chem.*, **21**, 510 (2008).
[8] A.C. Albeniz, D.M. Heinekey, R.H. Crabtree. *Inorg. Chem.*, **30**, 3632 (1991).
[9] J.T. Golden, R.A. Andersen, R.G. Bergman. *J. Am. Chem. Soc.*, **123**, 5837 (2001).

[10] S. Chen, G. Song, X. Li. *Tetrahedron Lett.*, **49**, 6929 (2008).
[11] S.R. Klei, J.T. Golden, T.D. Tilley, R.G. Bergman. *J. Am. Chem. Soc.*, **124**, 2092 (2002).
[12] S. Dagan, A. Amirav. *J. Am. Soc. Mass Spectrom.*, **7**, 550 (1996).
[13] T. Shima, Y. Sugimura, H. Suzuki. *Organometallics*, **28**, 871 (2009).
[14] S.K. Goforth, R.C. Walroth, L. McElwee-White. *Inorg. Chem.*, **52**, 5692 (2013).
[15] M. Thirumavalavan, P. Akilan, M. Kandaswamy. *Inorg. Chim. Acta*, **359**, 2555 (2006).
[16] Z.-M. Wang, B.-W. Sun, J. Luo, S. Gao, C.-S. Liao, C.-H. Yan, Y. Li. *Polyhedron*, **22**, 433 (2003).
[17] Y.-N. Chen, Y.-Y. Ge, W. Zhou, L.-F. Ye, Z.-G. Gu, G.-Z. Ma, W.-S. Li, H. Li, Y.-P. Cai. *Inorg. Chem. Commun.*, **14**, 1228 (2011).
[18] Y. Jin, Y. Qi, S.R. Batten, P. Cao, W. Chen, Y. Che, J. Zheng. *Inorg. Chim. Acta*, **362**, 3395 (2009).
[19] A. Castinñeiras, S. Balboa, R. Carballo, J. Niclós. *Z. Anorg. Allg. Chem.*, **628**, 2353 (2002).
[20] J.M. Rubin-Preminger, L. Kozlov, I. Goldberg. *Acta Cryst.*, **C64b**, m83 (2008).
[21] J. Černák, M. Kañuchová, J. Chomič, I. Potočňák, J. Kameníček, Z. Žák. *Acta Cryst.*, **C50**, 1563 (1994).
[22] J. Černák, E. Lengyelová, K. Ahmadi, A.-M. Hardy. *J. Coord. Chem.*, **37**, 55 (1996).
[23] H.L. Shyu, H.H. Wei, Y. Wang. *Inorg. Chim. Acta*, **258**, 81 (1997).
[24] Z.-E. Lin, J. Zhang, S.-T. Zheng, G.-Y. Yang. *Z. Anorg. Allg. Chem.*, **631**, 148 (2005).
[25] T. Korzeniak, C. Mathonière, A. Kaiba, P. Guionneau, M. Koziel, B. Sieklucka. *Inorg. Chim. Acta*, **361**, 3500 (2008).
[26] V. Aggarwal, S. Kashyap, U.P. Singh. *Open Crystallogr. J.*, **2**, 19 (2009).
[27] (a) Bruker AXS, *SMART, Version 5.631, Software Reference Manuals*, Bruker AXS GmbH, Karlsruhe, Germany (2000); (b) *SAINT, Version 6.63, Software Reference Manuals*, Bruker AXS GmbH, Karlsruhe, Germany (2000).
[28] G.M. Sheldrick. *Software for Empirical Absorption Correction: SADABS*, University of Göttingen, Göttingen, Germany (2001).
[29] (a) G.M. Sheldrick. *Program for Crystal Structure Solution: SHELXS-97*, University of Göttingen, Göttingen, Germany (1997); (b) G.M. Sheldrick. *Program for Crystal Structures Refinement: SHELXL-97*, University of Göttingen, Göttingen, Germany (1997).
[30] D. Bose, G. Mostafa, H.-K. Fun, B.K. Ghosh. *Polyhedron*, **24**, 747 (2005).
[31] A. Sabatini, I. Bertini. *Inorg. Chem.*, **4**, 959 (1965).
[32] C.L. Schmidt, M. Jansen. *Z. Anorg. Allg. Chem.*, **638**, 275 (2012).
[33] K.-Y. Choi, K.M. Chun, I.H. Suh. *J. Chem. Crystallogr.*, **28**, 831 (1998).
[34] O.V. Nesterova, S.R. Petrusenko, V.N. Kokozay, B.W. Skelton, J.K. Bjernemose, P.R. Raithby. *Inorg. Chim. Acta*, **358**, 2725 (2005).
[35] D.A. Oyugi, F.O. Ayorinde, A. Gugssa, A. Allen, E.B. Izevbigie, B. Eribo, W.A. Anderson. *J. Biosci. Tech.*, **2**, 287 (2011).
[36] G. Koehl, N. Keller, F. Garin, V. Keller. *Appl. Catal. A: Gen.*, **289**, 37 (2005).
[37] C. Ruiz-Pérez, P.A.L. Luis, F. Lloret, M. Julve. *Inorg. Chim. Acta*, **336**, 131 (2002).
[38] Y. Sasaki. *Bull. Inst. Chem. Res., Kyoto Univ.*, **58**, 187 (1980).